Journal of Beijing Institute of Technology, 2025, Vol. 34, No. 3

Preparation of Porous Poly (M-Phenylene Isophthalamide) Films with Reduced Dielectric Constants Using Wet Phase Inversion Method Optimization and Performance Evaluation

M. Abdelaty[1,2]✉, Huanhuan Zhu[1], Yun Zhao[1], Qingze Jiao[1,3]

(1. School of Chemistry and Chemical Engineering, Beijing Institute of Technology, Beijing 100081, China; 2. Faculty of Engineering, Pharos University in Alexandria, Alexandria 21521, Egypt; 3. College of Materials and the Environment, Beijing Institute of Technology, Zhuhai 519085, China)

Abstract: Poly (m-phenylene isophthalamide) (PMIA), a key aromatic polyamide, is widely used for its outstanding mechanical strength, high thermal stability, and excellent insulation properties. However, different applications demand varying dielectric properties, so tailoring its dielectric performance is essential. PMIA was first synthesized in this study, followed by introducing pores and developing porous PMIA films and PMIA-based composites with reduced dielectric constants. Porous PMIA films were fabricated using the wet phase inversion process with N, N-dimethylacetamide (DMAC) solvent and water as the non-solvent. The impact of casting solution composition and coagulation bath temperature on pore structures was analyzed. A film produced with 18% PMIA and 5% LiCl in a 35 ℃ coagulation bath achieved the lowest dielectric constant of 1.76 at 1 Hz, 48% lower than the standard PMIA film, which had a tensile strength of 18.5 MPa and an initial degradation temperature of 320 ℃.

Keywords: poly (m-phenylene isophthalamide) (PMIA); porous PMIA; wet phase inversion; dielectric constant

1 Introduction

Poly (m-phenylene isophthalamide) (PMIA), one of the aromatic polyamides, possesses superior flame retardancy, outstanding self-extinguishing characteristics, and ideal insulation ability [1–3]. The special molecular structure with abundant hydrogen bond networks endows PMIA with distinctive thermal stability and excellent mechanical properties [4, 5]. Due to such advantages, PMIA has been widely used in high-performance filter membranes, electrical insulation, flame retarded materials, energy storage application, and aerospace and protective clothing [6, 7].

PMIA materials exhibit better processability than inorganic solid-insulating materials commonly used in microelectronic fields. However, traditional PMIA shows dielectric constants of 2.3 to 3.5 and thus hardly serves as an insulation material with lower dielectric constants in microelectronic devices. Therefore, reducing the dielectric constant of PMIA and regulating its dielectric properties is necessary [8, 9].

Developing low-dielectric PMIA films significantly enhances their suitability for a wide range

Manuscript received Feb. 17, 2025; revised May 7, 2025; accepted May 10, 2025. The associate editor coordinating the review of this manuscript was Dr. Yixiao Gu.

✉ Corresponding author. Email: mahmoud.abdelaty@pua.edu.eg

DOI: 10.15918/j.jbit1004-0579.2025.010

of high-performance electronic and insulation applications. In flexible printed circuit boards (FPCBs), the reduced dielectric constant helps minimize signal loss and crosstalk, thereby improving signal integrity and transmission speed in compact, bendable devices. In high-frequency communication systems, such as fifth-generation (5G) and next-generation wireless technologies, low-k materials are essential for ensuring efficient signal propagation and reducing energy consumption. In the aerospace and defense sectors, PMIA is an ideal candidate for lightweight, high-performance insulation components capable of withstanding extreme environments. Additionally, in energy storage systems like capacitors and lithium-ion batteries, low-dielectric PMIA films function as critical insulating layers, enhancing energy density and safety by minimizing parasitic capacitance [10–12].

The reported approaches to lowering the dielectric constant of PMIA focus on introducing bulky groups or the trifluoromethyl group (CF3) groups in the molecular chain, which may increase the free volume of PMIA and further decrease the number of polarizable groups per unit volume. However, the problems lie in the complicated preparation process and the high cost [13, 14].

The low-k materials used are being constantly optimized to address two important issues: 1) to prevent leakage between wiring elements of the circuitry; 2) to minimize time delay losses in the wiring.

Time delays arise from parasitic capacitance deriving from the proximity of the wires and inter-wire field penetration. Resistive-capacitive (RC) coupling effectively increases the time taken for electrons to pass through the circuit. The delay time can be approximately written as follows

$$t_{RC} = 2\rho k\varepsilon_{\circ}(4L^2/P^2 + L^2/D^2) \qquad (1)$$

where $\varepsilon_{\circ}$ means a parameter or value that can change depending on conditions or experimental setup. In this case, ρ, which represents wire resistivity, can vary depending on the material of the wire, temperature, or manufacturing conditions. k stands for the material dielectric constant (or relative permittivity), P stands for wire resistivity, L stands for wire length, and D stands for the wire height. The time delay can be compared to the gate delay time, which is defined by the time it takes to charge the logic device. As devices have been miniaturized, the gate delay has continually decreased because the charge needed decreases with size, while the RC-related delay has increased because the pitch and diameter of wires have decreased [15].

Since air is the substance with the lowest dielectric constant of 1.0, introducing air into the polymer matrix is an attractive and reasonable approach to achieving low dielectric constant materials [16]. However, there are few reports on the dielectric constants of PMIA porous membranes.

Porous polymers have been prepared using several methods, including the use of blowing agents [17], thermally labile urethane prepolymers [18], and ceramic components [19]. Such methods require additives to generate pores in a polymer matrix, whereas a phase inversion process can provide asymmetric porous polymer films from a homogeneous polymer solution. Wet phase inversion processes are usually utilized by immersing a thin cast polymer solution into a non-solvent coagulation bath [20]. These porous films have wide-range pore diameters (from nanometers to micrometers), different pore structures (finger-like or sponge-like), and high porosity [21, 22].

During the past few years, several researchers have prepared porous PMIA membranes by the phase inversion process to improve their properties for different applications. Ren et al. [23] prepared a PMIA nanofiltration membrane for chromium (VI) removal through a phase inversion process. Lin et al. [24] prepared potential PMIA for breaking through the selectivity-permeability trade-off for ultrafiltration mem-

branes with various effective pore radii (6.58 nm, 6.84 nm, and 9.28 nm) via nonsolvent-induced phase separation. PMIA membrane exhibited high porosity, narrow pore radius distribution, and excellent hydrophilicity, leading to its high performance in the filtration process. Hejian Li et al. [25] fabricated nonsolvent-induced phase separation techniques using recyclable porous fluorinated polyimide films with adjustable. Porosities range from 33% to 71%. These films exhibit dielectric constants between 1.51 and 2.42 at 100 kHz, coupled with excellent thermal stability and mechanical properties, making them suitable. These films are suitable for high-frequency communication devices. Soohyun Kim et al. [26] utilized wet phase inversion to create porous polyimide membranes with a dielectric constant as low as 1.7. The process involved tailoring solvent/non-solvent compositions and coagulation conditions to achieve the desired porosity and dielectric properties. Wen Li et al. [27] fabricated carbon nitride/polyimide porous films via non-solvent induced phase separation (NIPS), achieving dielectric constants ranging from 1.56 to 2.50 at 1 MHz. The incorporation of porous structures and fluoroalkylsilane (FAS)-grafted fillers contributed to the reduced dielectric constants.

In this chapter, porous PMIA films were fabricated using a wet phase inversion process. The influence of PMIA concentrations in N, N-dimethylacetamide (DMAC), LiCl contents, and coagulation bath temperatures on the morphologies, mechanical strength, and dielectric constants of resultant PMIA porous films was systematically studied.

2 Experimental Parts

2.1 Materials

PMIA was prepared by interfacial polycondensation reaction in Beijing Institute of Technology. DMAC (> 99%) was supplied by Tian in Fuyu Fine Chemical Reagent Co., Ltd, China. Lithium chloride was supplied by Tianjin Guangfu Fine Chemical Reagent Co., Ltd, China. Lithium chloride was dried at 110 ℃ overnight before use.

2.2 Preparation of PMIA and Porous PMIA Films

The synthesis of PMIA was conducted in a 500 mL three-neck flask equipped with a mechanical stirrer. Aqueous-phase polymerization was initiated by adding a solution containing 5.41 g of m-phenylenediamine, 10.6 g of sodium carbonate, and 0.5 g of sodium lauryl sulfate in 145 mL of deionized water. To this, a separate solution of 10.66 g of isophthaloyl chloride in 180 mL of tetrahydrofuran (THF) was rapidly introduced with moderate stirring. The reaction mixture was agitated for 12 min to allow for interfacial polymerization. The resulting polymer was separated via filtration, thoroughly washed with deionized water and acetone, and dried at 100 ℃ in vacuum for 12 h.

Porous PMIA films were fabricated using a wet phase inversion technique, as schematically illustrated in Tab. 1 and Fig. 1. A homogeneous and transparent casting solution was prepared by

Tab. 1 Preparation parameters of PMIA films

Parameter	Setting/range	Purpose
PMIA concentration (wt%)	15–20	To control viscosity and polymer content
LiCl concentration (wt%)	3–7	Pore-forming agent for phase inversion
Solvent	DAMC	Dissolution medium for PMIA and LiCl
Dissolution temperature	80 ℃	To ensure complete solubilization
Degassing conditions	80 ℃ for 1 h	To remove trapped air bubbles in the casting solution
Glass plate and casting knife temperature	60 ℃	To prevent premature phase separation during casting
Casting knife gap	150 μm	To determine the initial film thickness
Pre-heating of wet film	95 ℃ for 10 min	To stabilize the film before coagulation
Coagulation bath temperature	25 ℃ – 45 ℃	To control pore size and structure
Coagulation medium	Deionized water	To initiate phase inversion
Washing conditions	24 h in deionized water	To remove residual LiCl and solvent

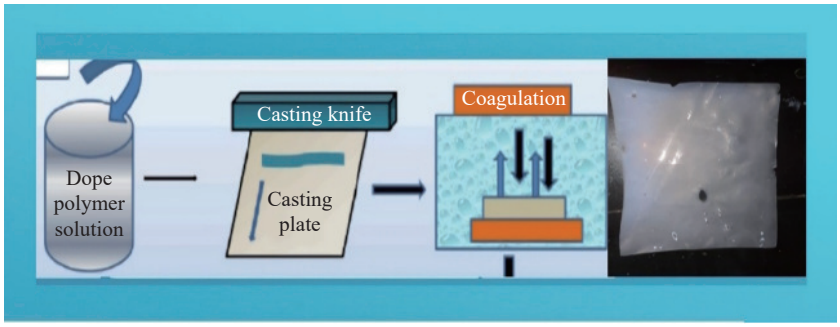

Fig. 1 The schematic illustration for the preparation of the PMIA film

dissolving PMIA (15 wt%–20 wt%) and lithium chloride (3 wt%–7 wt%) in DMAC at 80 ℃. The solution was degassed in an oven at 80 ℃ for 1 h before casting. Both the glass plate and casting knife were preheated to 60 ℃. The casting solution was then applied onto the glass plate and spread evenly using a casting knife with a 150 μm gap. The resulting wet film was pre-heated in an oven at 95 ℃ for 10 min and subsequently immersed in a water coagulation bath maintained at 25 ℃–45 ℃. After complete phase separation and solidification, the film was peeled off and washed thoroughly with deionized water for 24 h to remove residual solvent and lithium chloride.

For comparison, nonporous PMIA films were prepared by a dry casting process in identical thermal conditions (95 ℃), omitting the coagulation bath immersion step to eliminate pore formation.

2.3 PMIA Film Characterization

Fourier transform infrared (FTIR) spectra were performed on a Shimadzu IRAffinity-1s instrument using ultrathin polymer films.

The mechanical properties of PMIA films were measured on a universal testing machine (SERVO PULSER, Simadzu EFH-EB20-40 L) at ambient temperature and a crosshead speed of 5 mm/min. Five rectangular specimens of 40 mm length, 10 mm width, and 0.050 mm thickness were tested for every sample, and the average value was adopted.

The dielectric constants (k) of polymer films were measured using a Novocontrol Concept 80 broadband dielectric spectrometer in a frequency range of 1 Hz to 10^6 Hz at room temperature.

2.4 Results and Discussion

2.4.1 Formation Mechanism of Porous PMIA

Porous film formation using a wet phase inversion process is recognized as a phase separation process in which a homogeneous polymer solution is transformed into a two-phase system, i.e., a solid polymer-rich phase that forms the film structure and a liquid polymer-poor phase, which forms the film pores [28].

The three-component phase diagram of polymer-solvent-precipitant serves as a useful tool for discussing the thermodynamic aspects of the membrane precipitation process. A typical phase diagram is presented schematically in Fig. 2.

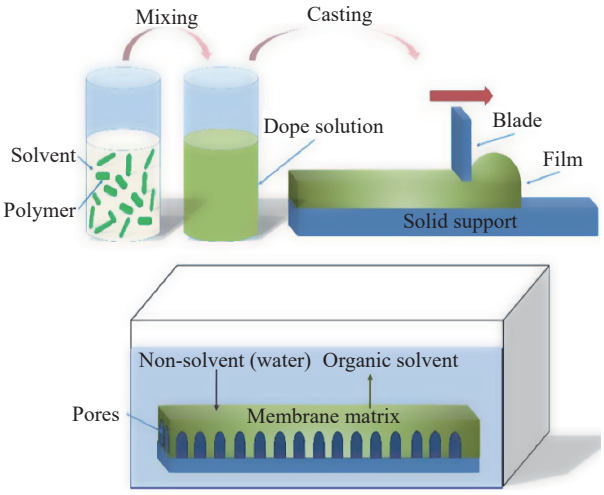

Fig. 2 Non-solvent phase inversion casting process [29]

The corners of the triangle represent the three components: polymer, solvent, and precipitant, while any point within the triangle represents a mixture of the three components. The

system consists of two regions: a one-phase region where all components are miscible and a two-phase region where the system separates into a polymer-rich, generally solid phase and a polymer-poor, generally liquid phase. Although the one-phase region in the phase diagram is thermodynamically continuous, for practical purposes it can conveniently be divided into a liquid and a solid region. Thus, at low polymer concentrations, the system is a low-viscosity liquid, but as the concentration of polymer is increased, the viscosity of the system also increases rapidly, reaching such high values where the system can be regarded as a solid. During membrane formation, the system changes from a composition A, which represents the initial casting solution, to a composition C, which represents the final membrane. At the composition C, two phases are in equilibrium, a solid phase which forms the membrane structure, represented by point S, and a liquid (polymer-poor) phase which constitutes the membrane pores filled with precipitant, represented by point L. Position C on line S-L determines the overall porosity of the membrane. The entire precipitation process is thus represented by the path A to C, during which the solvent is exchanged by the precipitant. Point B along the path is the concentration at which the first polymer precipitates. As precipitation proceeds, more solvent is lost, and the viscosity of the polymer-rich phase rises. At some point, the viscosity is high enough for the precipitated polymer to be regarded as a solid, and further bulk movement of the polymer is hindered. This composition is shown as D in Fig. 3. Volume changes produced by further solvent-precipitant exchange result in a shrinkage of the polymer-rich phase. It should be appreciated that the phase diagram is the description of an equilibrium state. It reflects the conditions in which a multicomponent mixture is stable, as a homogeneous phase or decays into two separate phases [29].

2.4.2 Structures of PMIA

As-synthesized PMIA shows an inherent viscosity of 2.1 dL/g. Its structure is confirmed by FTIR. The FTIR spectrum of PMIA is shown in Fig. 4. The absence of the acid chloride band at 1 770 cm^{-1} confirms the successful formation of PMIA. The peak at 3 290 cm^{-1} can be assigned to the *N-H* stretching vibrations in a secondary amide in the Transform with bonded hydrogen. The band at 3 000 cm^{-1} is due to the unsaturated *C-H* stretching vibration. The band at 1 650 cm^{-1} is ascribed to the amide *C=O* group for hydrogen-bonded amide groups. The group of closely related bands at 1 600 cm^{-1} can be attributed to aromatic *C=C* stretching. The band at 1 512 cm^{-1} indicates *N-H* in-plane bending and *C-N* stretching, and the band at 1 255 cm^{-1} indicates *C-N* stretching and *N-H* in-

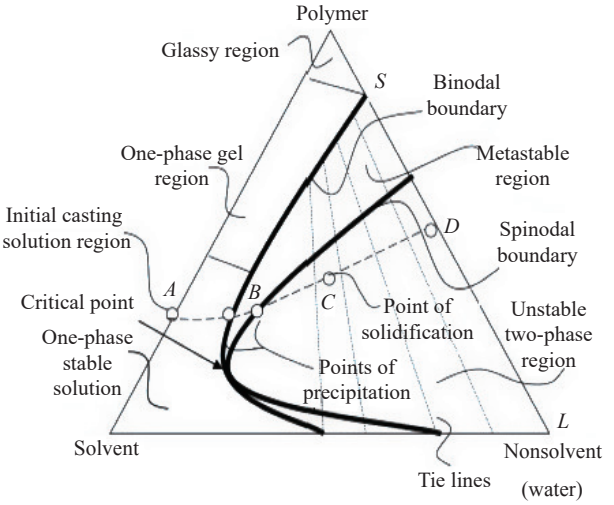

Fig. 3 Schematic phase diagram of the system polymer-solvent-precipitant showing the precipitation pathway of the casting solution during film formation [30]

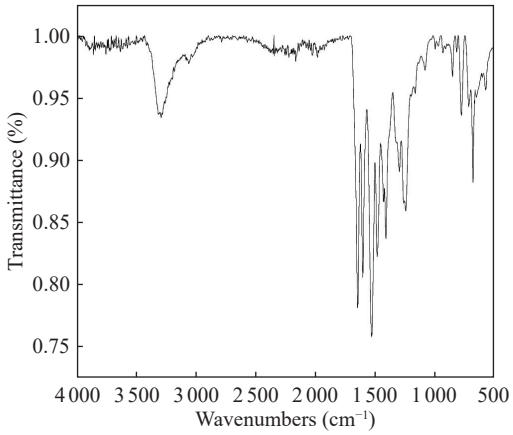

Fig. 4 FTIR spectrum of as-prepared PMIA

plane bending. Finally, the sharp bands at 770 cm^{-1} and 673 cm^{-1} are attributed to out-of-plane *C-H* vibrations of one and three adjacent hydrogens in a meta-substituted aromatic ring.

2.4.3 Morphologies of Porous PMIA Films

Aromatic polyamide polymer is not soluble in common solvents. The addition of inorganic salts like LiCl is necessary to enhance the solubility of the polymer in the amide-type of solvents, like DMAC. Different concentrations of the polymer and LiCl were added into a polar solvent, DMAC, and heated with agitation to complete dissolution.

As shown in Tab. 1, porous PMIA films were prepared by immersing wet PMIA films obtained with different casting solution compositions into a water coagulation bath in different temperatures. As exhibited in Fig. 5 (a), PMIA is a nonporous PMIA film obtained using a dry process without treatment in a water coagulation bath. Compared to PMIA 1, PMIA 2, and PMIA 3 (Tab. 1 and Fig. 5 (a), (b), (c), and (d), PMIA concentrations have effects on the pore size and the pore numbers on the film surface. PMIA 1 prepared using 15 wt% of PMIA concentration shows a porous surface with a pore diameter of 100 to 150 nm. While PMIA 2 obtained using 18 wt% of PMIA concentration displays a porous film with a large number of pores. The micropores are closed and have uniform and regular shapes, having a diameter of 100 to 300 nm. However, when PMIA content is increased to 20 wt%, the pore number of the film decreases a lot, and the pore size ranges from 100 nm to 500 nm.

The proposed pore size distribution is due to the lower diffusion rate of the non-solvent at a high solution viscosity. An increase in the polymer concentration results in a significant increase in the solution viscosity of the PMIA solution. This phenomenon will lead to a higher mass transfer resistance between the non-solvent (coagulation bath) and the solvent (DMAC) in the system during the solidification of the casting solution. Thus, at high polymer concentrations, the precipitation process stops after a longer period, which leads to the formation of a denser film with a smaller pore size distribution. The optimum concentration of PMIA for preparing porous films is 18 wt%.

PMIA 2, PMIA 4, and PMIA 5 in Tab. 2 and Fig. 5 (c), (e), and (f) show the influence of LiCl contents on the pore structures of PMIA films. PMIA 2 obtained using 3 wt% of LiCl shows a porous film with a large number of pores. When LiCl weight percent is 5%, the pore size and the number of large pores increase, but the network structure remains unchanged. The higher LiCl weight percent of 7% tends to decrease.

The radius and number of the network pores affect the overall porosity and mechanical strength of the film. This result is apparently due to the presence of larger amounts of nonsolvent swelling agent in the casting solution, which leads to the higher flux of gelation media into the film during the gelation process. The optimum concentration of LiCl for preparing porous films is 5 wt%.

The phase inversion was performed at 25 ℃, 35 ℃, and 45 ℃, respectively. As presented in Tab. 1 and Fig. 5 (e), (g), and (h), the pore sizes of the porous film (PMIA 4) formed using a casting solution of PMIA 18 wt% and LiCl 5 wt% with phase inversion in 25 ℃ are smaller and more homogenous than those (PMIA 6, PMIA 7) formed in 35 ℃ and 45 ℃. With the temperature, the pores became larger and longer. Such a phenomenon is generated from the nature of phase inversion, saying that the solvent exchange of DMAC in the polymeric solution and water in the coagulation bath is quick at a higher temperature. The process of phase separation is accelerated while the precipitation of the polymer is delayed.

2.4.4 Dielectric Constants of Porous PMIA Films

The k value of porous low-k dielectrics depends

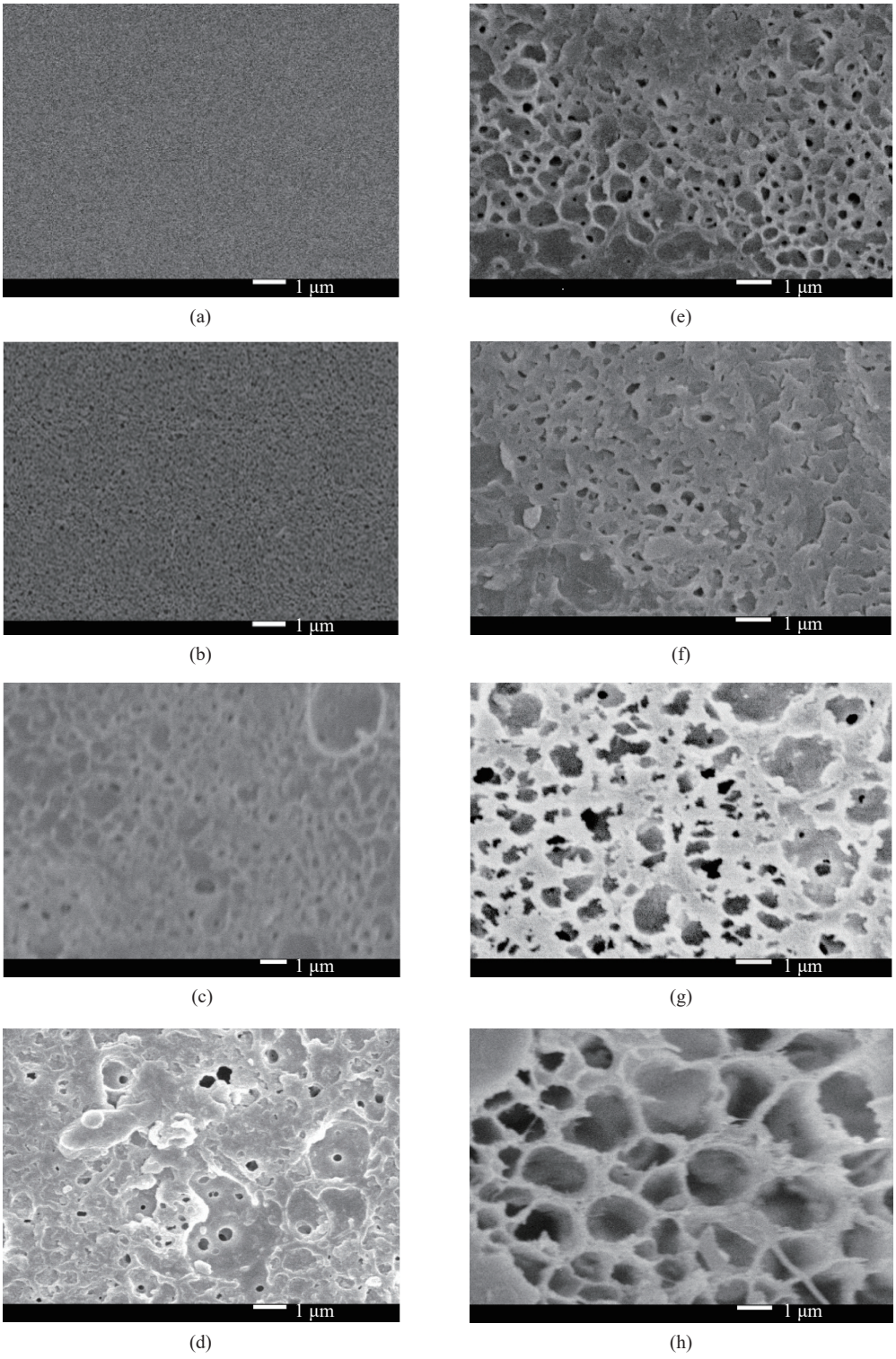

Fig. 5 Scanning electron microscopy (SEM) images of the surface of as-prepared PMIA films: (a) dry process PMIA; (b) PMIA 1; (c) PMIA 2; (d) PMIA 3; (e) PMIA 4; (f) PMIA 5; (g) PMIA 6; (h) PMIA 7

on the porosity and dielectric constant of the film skeleton (k_2)

$$\frac{k-1}{k+2} = V\frac{k_1-1}{k_1+2} + (1-V)\frac{k_2-1}{k_2+2} \qquad (2)$$

where k_1 is the dielectric constant of the material inside the pores, and V is the average pore volume. The first term on the right side of the equation equals zero if the air is inside the pore (k_1-

Tab. 2 Preparation conditions and characteristics of PMIA films

Sample	Casting solution composition (wt%)			Coagulation bath temperature (℃)	Pore size of porous films (nm)
	PMIA	LiCl	DMAC		
PMIA 1	15	3	82	25	100 – 150
PMIA 2	18	3	79	25	100 – 300
PMIA 3	20	3	77	25	100 – 500
PMIA 4	18	5	77	25	100 – 250
PMIA 5	18	7	75	25	100 – 400
PMIA 6	18	5	77	35	150 – 800
PMIA 7	18	5	77	45	>1000

1.0). As a result, porous low-k dielectrics with relatively small k_2 values and higher porosity can provide a much lower k value [31].

The dielectric constants (k) of different PMIA films in the range of 1 Hz to 106 Hz are shown in Fig. 6. The k decreases with increasing frequency for all samples. Those samples, except PMIA 1, obtained using the wet phase inversion method, show a smaller k in almost the whole frequency range than the PMIA film produced by a dry process. It can be seen that k varies with the content of PMIA in the film-casting solution Fig. 4. The k for PMIA at 1 Hz is 3.44, while the k of PMIA 1, PMIA 2, and PMIA 3 are 3.10, 2.40, and 2.61 at 1 Hz, respectively. The porous PMIA 2 film with a uniform and large number of pores obtained using 18 wt% PMIA concentration shows the dielectric constant of 2.43 at 1 Hz. As shown in Fig. 3 and Fig. 4, the content of LiCl in the film casting solution also influences the k of PMIA films. The k of PMIA 2, PMIA 4, and PMIA 5 are 2.40, 2.05, and 2.22 at 1 Hz, respectively. The porous PMIA 4 film with larger pore sizes and numbers obtained using 5 wt% LiCl concentration shows the dielectric constant of 2.05 at 1 Hz. As presented in Fig. 6, the coagulation bath temperatures affect the k of porous PMIA films. The k of PMIA 4, PMIA 6, and PMIA 7 are 2.05, 1.76, and 1.91 at 1 Hz, respectively. The results indicate that PMIA 6 with many larger sizes of pores shows the lowest k of 1.76. It indicates that the dielectric properties of PMIA films can be controlled to some extent by varying the concentration of the casting solution composition and the coagulation bath temperature. In summary, the PMIA concentration, LiCl content, and coagulation bath temperature have effects on the number and sizes of pores for PMIA films, which lead to the difference in dielectric constants.

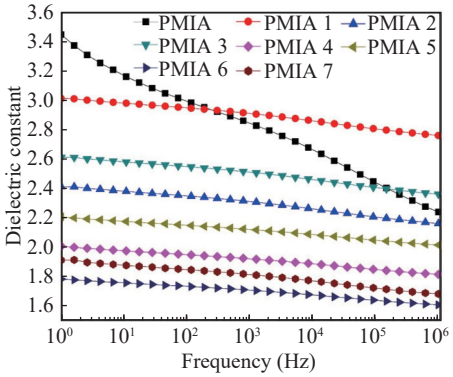

Fig. 6 The dielectric constants of as-prepared PMIA films with different PMIA compositions, with different LiCl contents, and in different coagulation bath temperatures

2.4.5 Thermal Properties of Porous PMIA Films

The thermal stability of PMIA and PMIA 6 was evaluated using thermogravimetric analysis (TGA) under a nitrogen atmosphere. The TGA results are shown in Fig. 7. It can be easily observed that the degradation is shifted to lower temperatures of 320 ℃ for PMIA 6. There is a slightly negative effect on thermal stabilization. Therefore, PMIA 6 shows lower thermal stability. It can be illustrated that porous structures in composite films can reduce the heat resistance of the film slightly.

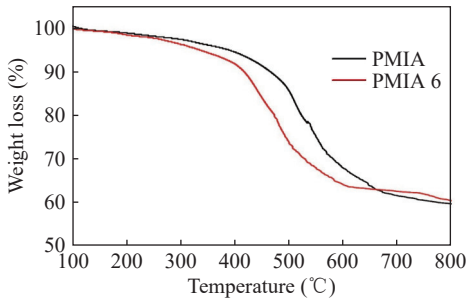

Fig. 7 TGA curve of as-synthesized PMIA and PMIA 6

2.4.6 Mechanical Properties of Porous PMIA Films

The mechanical properties of as-obtained PMIA

films at a fixed casting thickness (0.3 mm) are shown in Fig. 8. The elongation at break of PMIA and PMIA 6 is 22.5 % and 17.5%, respectively. PMIA 6 shows a lower tensile strength of 18 MPa as a result of the effect of the wet phase inversion process compared with PMIA with the dry process. It indicates that the introduction of pores in PMIA films decreases the mechanical performance.

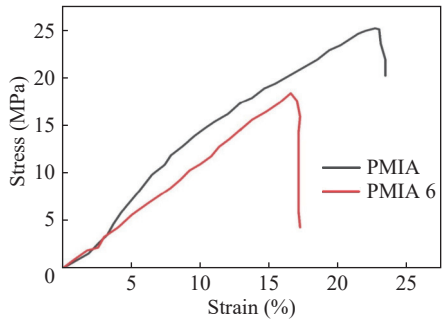

Fig. 8 Stress-strain curve of as-prepared PMIA and PMIA 6 films

3 Conclusion

The porous PMIA films were fabricated using the wet phase inversion process based on a solvent/non-solvent system. DMAC served as the solvent, while water functioned as the non-solvent coagulation bath. The effects of the casting solution composition and the coagulation bath temperature on the pore structures of PMIA films were investigated. The porous PMIA film obtained with a casting solution of 18% PMIA and 5% LiCl, combined with a coagulation bath of 35 ℃, exhibits the lowest dielectric constant of 1.76 at 1 Hz, which is 48% lower than the 3.44 dielectric constant of the PMIA standard film. This porous PMIA film has a tensile strength of 18.5 MPa and an initial degradation temperature of 320 ℃.

4 Future Work

To elaborate on the current study and support the development of low-dielectric PMIA materials for practical applications, several key research directions are proposed. First, the porosity of PMIA films will be further optimized using advanced pore-forming agents and templating methods to fine-tune both dielectric and mechanical properties with greater precision. The incorporation of nanomaterials, such as boron nitride and graphene, into PMIA matrices will be explored to develop hybrid composites that simultaneously achieve low dielectric constants, high thermal conductivity, and improved mechanical robustness. In parallel, long-term performance will be evaluated through durability testing in various environmental conditions, including thermal aging, moisture absorption, and mechanical fatigue, to ensure reliability in service. Lastly, the scalability of the fabrication process will be investigated, with a focus on adapting laboratory techniques for industrial-scale production, paving the way for commercial implementation in electronics, aerospace, and energy systems.

References:

[1] W. Volksen, R. Mille, and G. Dubois, "Low dielectric constant materials, " *Chemical Review*, vol. 110, pp. 56-110, 2010.

[2] S. Chisca, V. Musteata, and I. Sava, "Dielectric behavior of some aromatic polyimide films, " *European Polymer Journal*, vol. 47, pp. 1186-1199, 2011.

[3] S. Fu, Y. Sun, W. Huang, Y. Li, and Y. Hu, "Some basic aspects of polymer nanocomposites: A critical review, " *Nano Materials*, vol. 1, pp. 89-106, 2019.

[4] G. Duan, Y. Wang, J. Yu, J. Zhu, and Z. Hu, "Improved thermal conductivity and dielectric properties of flexible PMIA composites via building interconnected boron nitride networks, " *Frontiers of Materials Science*, vol. 13, pp. 64-76, 2019.

[5] A. Venkatesan and R. Gopalan, "Polymers and polymer matrix nanocomposites for high performance dielectric applications: A review, " *Materials Today: Proceedings*, vol. 39, pp. 960-966, 2021.

[6] M. Abdelaty, A. Soliman, and T. Taha, "In situ synthesis of PMIA/SiO_2 nanocomposites and porous PMIA films for high-temperature insulation applications," *Journal of Materials Science*: *Mate-*

rials in Electronics, vol. 36, pp. 1-12, 2025.

[7] Z. He, X. Shi, and S. Zhang, "Recent advances in polymer nanodielectrics: Fabrication, characterization, and modeling, " *Journal of Materials Science: Materials in Electronics*, vol. 30, pp. 1438-1456, 2019.

[8] T. Ohki, "Dielectric properties of polymer nanocomposites, " *IEEE Transactions on Dielectrics and Electrical Insulation*, vol. 17, no. 4, pp. 1029-1034, 2010.

[9] P. Sharma and N. Khare, "Dielectric properties of polymer nanocomposites, " *Materials Science and Engineering: B*, vol. 262, pp. 114692, 2020.

[10] A. Panda, B. Behera, and B. Jena, "Dielectric and electrical properties of polymer nanocomposites: A review, " *Materials Today: Proceedings*, vol. 33, pp. 5605-5609, 2020.

[11] J. Li, X. Zhang, Z. Wu, Y. Zhang, and X. Zhang, "Interface design and dielectric performance in polymer-based dielectric composites, " *Composites Science and Technology*, vol. 196, pp. 108222, 2020.

[12] A. George and S. Thomas, "Dielectric materials for electrical engineering applications, " *Composites Part B: Engineering*, vol. 43, no. 3, pp. 1159-1168, 2012.

[13] H. Deng and M. Liu, "Polymer-based dielectric composites for electronic packaging: A review, " *Composites Part A: Applied Science and Manufacturing*, vol. 124, pp. 105502, 2019.

[14] Y. Zhang, G. Yang, Y. Bai, Y. Wang, and Z. Liu, "Improved dielectric properties of polyimide-based nanocomposites via interface engineering, " *Polymer*, vol. 153, pp. 507-515, 2018.

[15] L. Cao, B. Huang, and Z. Guo, "Dielectric polymer composites with high permittivity for capacitor applications: A review, " *Composites Science and Technology*, vol. 169, pp. 110-124, 2019.

[16] R. Zhang, J. Guo, and Y. Wu, "High-performance dielectric polymer composites for energy storage: A review, " *Journal of Materials Chemistry A*, vol. 8, pp. 6410-6430, 2020.

[17] J. Wang, Y. Li, and Y. Yang, "Dielectric properties of polymer composites with high dielectric constant fillers: A review, " *Composites Part B: Engineering*, vol. 175, pp. 107070, 2019.

[18] S. Wang, M. Wang, and X. Liu, "High dielectric constant polymer composites: A review, " *Polymer Composites*, vol. 39, no. S3, pp. E2329-E2346, 2018.

[19] L. Zhang, J. Liang, and Z. Wu, "Recent advances in high dielectric constant polymer nanocomposites: Preparation, mechanisms, and applications, " *Materials Today Physics*, vol. 15, pp. 100265, 2020.

[20] M. Yao, J. Wang, and Q. Zhang, "A review of high dielectric constant polymer composites: Materials, structures, and applications, " *Composites Part B: Engineering*, vol. 202, pp. 108428, 2020.

[21] H. Lee and M. Cho, "Recent progress in dielectric polymer composites for energy storage applications, " *Nano Energy*, vol. 60, pp. 257-272, 2019.

[22] Y. Wang, L. Zhang, and X. Chen, "Dielectric polymer composites with high energy density and low dielectric loss, " *Advanced Materials*, vol. 32, no. 15, pp. 1904423, 2020.

[23] Q. Chen, Y. Wang, and W. Li, "Tailoring the interface in polymer-based dielectric composites, " *Progress in Materials Science*, vol. 103, pp. 94-135, 2019.

[24] B. Chu, X. Zhou, K. Ren, Q. Li, Y. Xiong, C. Zha, J. Yang, Q. Pei, and Y. Yang, "A dielectric polymer with high electric energy density and fast discharge speed, " *Science*, vol. 313, pp. 334-336, 2006.

[25] H. Liu, M. Lin, and Y. Xu, "Polymer-based nanocomposites with high dielectric performance: A review, " *Composites Part A: Applied Science and Manufacturing*, vol. 140, pp. 106171, 2021.

[26] Y. Lin, H. Zhan, and Y. Wang, "Dielectric materials for electrical energy storage: Design, properties, and applications, " *Advanced Functional Materials*, vol. 29, no. 14, pp. 1807245, 2019.

[27] J. Zhang, X. Li, and L. Xu, "Surface modification of nanoparticles for polymer nanocomposites, " *Materials*, vol. 12, no. 19, pp. 3101, 2019.

[28] H. Kim, C. Lee, J. Oh, S. Yoon, and M. Park, "Enhancement of dielectric and thermal properties of epoxy composites by surface-modified alumina, " *Composites Part B: Engineering*, vol. 132, pp. 61-70, 2018.

[29] T. Takeuchi, T. Yano, and M. Enokida, "Surface modification of inorganic fillers for polymer composites, " *Applied Surface Science*, vol. 441, pp. 1040-1045, 2018.

[30] M. Sulaiman, N. Ismail, and R. Ahmad, "Surface functionalization of fillers for polymer composites: A review, " *Journal of Applied Polymer Science*, vol. 137, no. 33, pp. 48983, 2020.

[31] G. Li, Y. Liu, M. Zhang, Q. Li, L. He, Y. Wang, H. Zhang, and Q. Wang, "Interface design and enhancement of dielectric performance in polymer nanocomposites, " *Advanced Materials*, vol. 30, no. 22, pp. 1705515, 2018.

M. Abdelaty is a Ph.D. candidate and Lecturer at the Petrochemical Engineering Department, Pharos University in Alexandria, Egypt, majoring in gas and petrochemicals engineering with a strong academic foundation and a deep passion for research, teaching, and technological innovation, dedicated to advancing the field of materials science and engineering.

Huanhuan Zhu is a Ph.D. candidate majoring in chemical engineering and technology at School of Chemistry and Chemical Engineering, Beijing Institute of Technology, China. She works in aromatic polyamide copolymers and electromagnetic microwave absorbers. She has published 10 papers in these areas.

Yun Zhao is an Associate Professor at School of Chemistry and Chemical Engineering, Beijing Institute of Technology, China. Her research interests are mainly in nanomaterials and polymer/inorganic nanocomposites. She is engaged in controllable synthesis, structure, properties, and application of graphene, carbon nanotubes, doped carbon nanotubes, Nb_2O_5, TiO_2, composite oxides, and layered double hydroxides. In addition, her research is also focused on polymer/nanomaterial composites. She has published more than 150 papers and patents in these areas.

Qingze Jiao is a Professor at School of Chemistry and Chemical Engineering, Beijing Institute of Technology, China. His research interests are mainly on catalysts, functional nanomaterials, and polymer/inorganic nanocomposites. He is engaged in the polymer/nanomaterial composites, including PI/CNT nanocomposites, ABS/CNT/ferrite composites, and PET/LDH nanocomposites. He has published more than 200 papers and patents in these areas.